

ABCD-treatment of a propagating doughnut beam generated by a spiral phase plate

A. Mawardi,² S. Hild,¹ A. Widera,³ and D. Meschede^{1,*}

¹Institut für Angewandte Physik, Universität Bonn, Wegelerstr. 8, 53115 Bonn, Germany

²School of Microelectronic Engineering, Universiti Malaysia Perlis, 02600 Perlis, Malaysia

³Fachbereich Physik and Forschungszentrum OPTIMAS, Technische Universität Kaiserslautern, 67663 Kaiserslautern, Germany

*meschede@uni-bonn.de

Abstract: We apply the Collins-Huygens integral to analytically describe propagation of a doughnut beam generated by a spiral phase plate. Measured beam profiles in free space and through an ABCD-lens system illustrate excellent agreement with theory. Applications range from the creation of optical beams with angular momentum to microscopy to trapping neutral atoms. The method extends to other beam shaping components, too.

© 2011 Optical Society of America

OCIS codes: (050.4865) Optical vortices; (070.2580) Paraxial wave optics; (070.2590) ABCD transforms; (080.2730) Matrix methods in paraxial optics; (080.4865) Optical vortices

References and links

1. T. A. Klar, S. Hell, "Subdiffraction resolution in far-field fluorescence microscopy," *Opt. Lett.* **24**, 954 (1999)
2. T. Kuga et al., "Novel Optical Trap of Atoms with a Doughnut Beam," *Phys. Rev. Lett.* **78**, 4713 (1997)
3. A. Kaplan, N. Friedman, N. Davidson, "Optimized single-beam dark optical trap," *J. Opt. Soc. Am. B* **19**, 1233 (2002)
4. P. Xu, X. He, J. Wang, M. Zhan, "Trapping a single atom in a blue detuned optical bottle beam trap", *Opt. Lett.* **35**, 2164 (2010)
5. D. W. Zhang, X.-C. Yuan, "Optical doughnut for optical tweezers," *Opt. Lett.* **28**, 740 (2003)
6. L. Allen, S. M. Barnett, M. J. Padgett, *Optical Angular Momentum*, Taylor and Francis, (2003)
7. M.R. Dennis, K. O'Holleran, M.J. Padgett, in "Progress in Optics," **53**, 293-363 (2009)
8. V. Y. Bazhenov, M. S. Soskin, M. V. Vasnetsov, "Screw dislocations in light wavefronts", *J. Mod. Opt.* **39**, 985 (1992)
9. N. R. Heckenberg, R. McDuff, C. P. Smith, A. G. White, "Generation of optical phase singularities by computer-generated holograms," *Opt. Lett.* **17**, 221 (1992)
10. E. Abramochkin, V. Volostnikov, "Beam transformations and nontransformed beams," *Opt. Commun.* **83**, 123 (1991)
11. M. Padgett, J. Arlt, N. Simpson, L. Allen, "Optical tweezers and optical spanners with Laguerre-Gaussian modes," *Am. J. Phys.* **64**, 77 (1996)
12. S. N. Khonina, V. V. Kotlyar, M. V. Shinkaryev, V. A. Soifer, G. V. Uspleniev, "The phase rotor filter," *J. Mod. Opt.* **39**, 1147 (1992)
13. M.W. Beijersbergen, et. al., "Helical-wavefront laser beams produced with a spiral phaseplate," *Opt. Commun.* **112**, 321 (1994)
14. J. H. Goodman, *Introduction to Fourier Optics* (McGraw-Hill, New York, 1968)
15. D. Rozas, C. T. Law, G. A. Swartzlander, "Propagation Dynamics in Optical Vortices," *J. Opt. Soc. Am. B* **14**, 3054 (1997)
16. Z. S. Sacks, D. Rozas, G. A. Swartzlander, "Holographic formation of optical-vortex filaments," *J. Opt. Soc. Am.* **15**, (1998)
17. S. A. Collins, Jr., "Lens-System Diffraction Integral Written in Terms of Matrix Optics," *J. Opt. Soc. Am.* **60**, 1168 (1970); A. Siegman, *Lasers*, University Science Books (Mill Valley 1986), p. 781
18. I. S. Gradshteyn, I. M. Ryzhik, *Table of Integrals, Series, and Products*, Academic Press (San Diego 1979)

1. Introduction

Optical beams with a dark spot at the center are called doughnut beams. They have proven useful for applications in high-precision imaging of biological samples [1], for trapping dark field seeking neutral atoms in blue detuned dipole traps [2, 3, 4], or with optical tweezers [5]. In recent years, also light beams carrying orbital angular momentum exhibiting a natural dark spot at their center have received increased interest [6, 7]. Methods for generating doughnut shaped beams include the use of computer-generated holograms [8, 9], cylindrical lens mode converters [10, 11] and the use of spiral phase plates (SPP) [12, 13].

Here we focus on doughnut beams generated by transforming a Gaussian beam with an SPP. From a practical point of view an analytic description compatible with the standard ABCD-formalism remains most favorable for the treatment of beam propagation. Since the transformed beam is not an eigen solution of the paraxial wave equation, a more elaborate treatment e.g. in terms of the paraxial Fresnel integral [14] is required. It was first studied theoretically in [15], and Fresnel type beam patterns were analyzed in [16]. The equivalent of the paraxial Fresnel integral in terms of the ABCD formalism is the Collins-Huygens integral [17] which we explicitly calculate. We furthermore illustrate its compatibility with the ABCD formalism by profile measurements of a Gaussian beam transformed by an SPP element.

2. Propagation dynamics of a doughnut beam

SPP components are commercially available for any optical wavelength. They consist of a cylindrical dielectric element with optical thickness increasing linearly with the azimuth angle ϕ . The SPP imprints a phase factor $\exp(i\ell\phi)$ onto incident beams, where in applications the most frequently used winding number or topological charge is $\ell = 1$. In the far field, cylindrically symmetric beams such as Gaussian beams are transformed into doughnut beams since all beam elements on opposing sides of the axis contribute with opposite sign and hence interfere destructively on the axis.

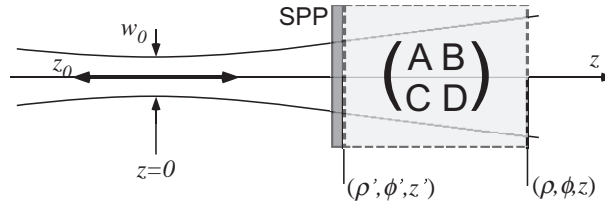


Fig. 1. A Gaussian beam is converted at position z' by a spiral phase plate (SPP). We are seeking the field distribution of the optical beam at position z in terms of the ABCD-coefficients of its trajectory.

For an incident centered Gaussian TEM_{00} beam centered on the SPP with negligible thickness and winding number ℓ at position z' (Fig. 1) the field amplitude with maximal amplitude \mathcal{E}_0 directly behind the SPP takes for cylindrical coordinates (ρ', ϕ', z') the form

$$E(\rho', \phi', z') = \mathcal{E}_0 \frac{w_0}{w(z')} \exp\left[-\frac{\rho'^2}{w^2(z')}\right] \exp\left[-ikz' - i\frac{k\rho'^2}{2R(z')} + i\eta(z')\right] \exp(i\ell\phi'). \quad (1)$$

The wave number is $k = 2\pi/\lambda$ and w_0 and $z_0 = \pi w_0^2/\lambda$ designate the $1/e$ -waist and the half-Rayleigh length of the incoming Gaussian beam, respectively. We have $R(z') = z'(1 + (z_0/z')^2)$, $w^2(z') = w_0^2(1 + (z'/z_0)^2)$, and $\eta(z') = \tan^{-1}(z'/z_0)$ the Gouy phase.

For a conventional Gaussian beam (i.e. for $\ell = 0$) the field distribution $E(\rho, \phi, z)$ can be calculated once the parameters $R(z)$ and $w(z)$ at position z are evaluated in terms of ABCD-

matrices involving all components acting on the propagating optical beam in between z' and z . For a Gaussian beam transformed by a spiral phase plate (SPP) ($\ell \geq 1$) this no longer the case. Collins has shown [17], however, that the ABCD formalism remains very useful in the paraxial approximation: The Collins-Huygens integral

$$E(\rho, \phi, z) = -\frac{i}{\lambda B} \exp(ikz) \int_0^\infty \int_0^{2\pi} E(\rho', \phi', z') \exp\left[\frac{ik}{2B}(A\rho'^2 + D\rho^2)\right] \exp\left[\frac{-ik\rho\rho' \cos(\phi - \phi')}{B}\right] \rho' d\rho' d\phi'. \quad (2)$$

allows to calculate the field distribution $E(\rho, \phi, z)$ for any known initial distribution $E(\rho', \phi', z')$ as a function of the global ABCD coefficients characterizing propagation from z' to z . Substituting Eq. (1) into Eq. (2), we find

$$E(\rho, \phi, z) = -\frac{i}{\lambda B} \mathcal{E}_0 \frac{w_0}{w(z')} \exp\left(\frac{ikD\rho^2}{2B}\right) \exp[ik(z - z')] \exp[i\eta(z')] \times \int_0^\infty \int_0^{2\pi} \exp\left[\frac{-\rho'^2}{w^2(z')} - i\frac{k\rho'^2}{2R(z')} + i\frac{kA\rho'^2}{2B}\right] \exp\left[\frac{-ik\rho\rho' \cos(\phi - \phi')}{B}\right] \exp(i\ell\phi') d\phi' \rho' d\rho' \quad (3)$$

For the sake of clarity we introduce abbreviations

$$E_{00}(\rho, z') = \mathcal{E}_0 \frac{w_0}{w(z')} \exp\left(\frac{ik\rho^2}{2B/D}\right) \exp(-ikz') \exp[i\eta(z')], \quad (4)$$

which represents a Gaussian TEM₀₀-mode with

$$\frac{1}{R_C^2(z')} = \left[\frac{1}{w^2(z')} + \frac{ik}{2R(z')} - \frac{iAk}{2B} \right] \quad \text{and} \quad 1/\rho_C = k\rho/B, \quad (5)$$

yielding an effective Collins curvature radius R_C , and a radius ρ_C characterizing the extension of the vortex structure. Re-writing Eq. (3) we find

$$E(\rho, \phi, z) = -\frac{i}{\lambda B} \exp(ikz) E_{00}(\rho, z') \times \int_0^\infty \int_0^{2\pi} \exp\left[-\frac{\rho'^2}{R_C^2(z')}\right] \exp\left[-i\frac{\rho'}{\rho_C} \cos(\phi - \phi')\right] \exp(i\ell\phi') d\phi' \rho' d\rho'. \quad (6)$$

Azimuthal integration over ϕ' yields an ℓ -th order Bessel function of the first kind:

$$E(\rho, \phi, z) = \frac{2\pi(-i)^{|\ell|+1}}{\lambda B} E_{00}(\rho, z') \exp(ikz) \exp(i\ell\phi) \int_0^\infty \exp[-\rho'^2/R_C^2(z')] J_\ell(\rho'/\rho_C) \rho' d\rho'. \quad (7)$$

The integral can be expressed in terms of modified Bessel functions I_m of the first kind and m -th order using the formula[18]

$$\int_0^\infty x \exp(-\alpha x^2) J_\nu(\beta x) dx = \frac{\sqrt{\pi}\beta}{8\alpha^{3/2}} \exp\left(-\frac{\beta^2}{8\alpha}\right) \left[I_{\frac{1}{2}|\nu|-\frac{1}{2}}\left(\frac{\beta^2}{8\alpha}\right) - I_{\frac{1}{2}|\nu|+\frac{1}{2}}\left(\frac{\beta^2}{8\alpha}\right) \right]. \quad (8)$$

Identifying $\alpha = 1/R_C^2$ and $\beta = 1/\rho_C$ we find the analytic expression for the field amplitude propagated through the optical system from z' to z

$$E(\rho, \phi, z) = 2\pi^{3/2}(-i)^{|\ell|+1} \frac{E_{00}(\rho, z') R_C^3(z')}{8\rho_C \lambda B} \times \exp(ikz) \exp(i\ell\phi) \exp\left(-\frac{R_C^2}{8\rho_C^2}\right) \times \left[I_{\frac{1}{2}|\ell|-\frac{1}{2}}\left(\frac{R_C^2}{8\rho_C^2}\right) - I_{\frac{1}{2}|\ell|+\frac{1}{2}}\left(\frac{R_C^2}{8\rho_C^2}\right) \right]. \quad (9)$$

With parameters Eq. (4-5) and the analytic expression Eq. 9 the propagation of a paraxial doughnut beam through any $ABCD$ optical system is fully characterized. The beam profile can be calculated at any position, resulting in a convenient tool to analyze the propagation and focusing properties of doughnut beams generated by an SPP. Formula Eq. (9) is fully equivalent with the result derived first in [15].

3. Comparison with an experimental doughnut beam created by an SPP

We have experimentally investigated the propagation of a doughnut beam formed by an SPP for two important cases: propagation in free space and propagation through a lens system. A commercial SPP (RPC Photonics) produced by a lithographic technique imposes a phase factor $\exp(i\phi)$ with winding number $\ell = 1$ on an incident beam with wavelength of 849.9 nm.

We have used a standard setup to measure the beam profile, see Fig. 2. We filter the mode profile by a single mode optical fiber in order to prepare a clean Gaussian TEM_{00} beam. After the fiber the laser power is approximately $7.5 \mu\text{W}$ and the beam is linearly polarized. The beam is then passed through the SPP to generate the donut beam.

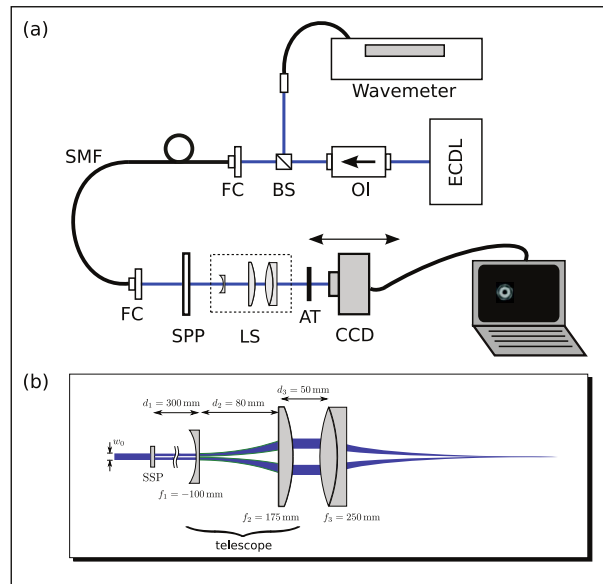


Fig. 2. (a): Setup for measuring the beam profile of the propagating doughnut beam in free space. (b): Details of the Galileian telescope used for the test measurement. *Abbreviations:* AT: attenuator; BS: beam splitter; CCD: beam profile camera; ECDL: external cavity diode laser; FC: fiber coupler; LS: lens system; OI: optical isolator; SMF: single-mode fiber; SPP: spiral phase plate. *Parameters:* $d_{1-3} = 300, 80, 50$ mm; $f_{1-3} = -100, 175, 250$ mm.

The beam profile of the generated donut beam is measured using a Spiricon camera and analyzed using its software. A typical image of the generated donut beam detected by the beam profile camera is shown in Fig. 3. From the recorded images a radial intensity distribution is extracted from a single transverse cut showing the doughnut character of the beams. The theoretical description according to Eq. (9) compares well at the % -level with the measurement where small asymmetries can be traced to small misalignments.

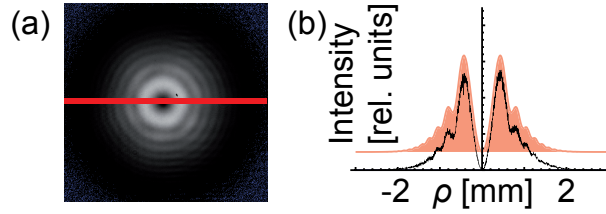


Fig. 3. (a): Beam profile at $z = 250$ mm for free space propagation. The 1D radial intensity distribution of the doughnut beam is taken along a straight line passing through the beam center (red line). (b): Radial intensity distribution extracted from the measurement. The theoretical curve (shaded area, shifted) shows all the details of the measured profile.

3.1. Propagation in free space

In free space, propagation of the beam through the distance z is given by the ray transfer matrix

$$\begin{pmatrix} A & B \\ C & D \end{pmatrix} = \begin{pmatrix} 1 & z \\ 0 & 1 \end{pmatrix} \quad (10)$$

for a distance z . The parameters (5) are

$$\frac{1}{R_C^2(z')} = \left[\frac{1}{w^2(z')} + \frac{ik}{2R(z')} - \frac{ik}{2z} \right] \quad \text{and} \quad 1/\rho_C = k\rho/z. \quad (11)$$

Insertion into Eq. 9 yields for free space propagation and $\ell = 1$

$$E(\rho, \phi, z) = -2\pi^{3/2} \frac{E_{00}(\rho, z') R_C^3(z')}{8\rho_C \lambda z} \exp(ikz) \exp(i\phi) \exp\left(-\frac{R_C^2}{8\rho_C^2}\right) \left[I_0\left(\frac{R_C^2}{8\rho_C^2}\right) - I_1\left(\frac{R_C^2}{8\rho_C^2}\right) \right]. \quad (12)$$

The variation of the 1D radial intensity distributions of the doughnut beam with distance in free space from the SPP was measured by removing the lens system from Fig. 2. The results are shown in Fig. 4 and compared with the numerically calculated intensity distributions. They agree very well at all distances. The beam profile undergoes significant changes upon propagation since the distances cover a range from the Fresnel diffraction limit to the Fraunhofer limit. At the beginning the beam shows a high peak intensity and several radial fringes. As the beam propagates the peak intensity decreases and the fringes disappear towards large radii.

3.2. Lens system

In order to illustrate the propagation of the beam through a lens system, we have chosen the configuration shown in Fig. 2(b) which is used in another experiment in our group to generate tightly focused dipole traps for neutral atoms. The ABCD-transfer matrix of the lens system is obtained by taking the product of the transfer matrices of the individual optical elements, $\mathbf{M}_{\text{tot}} = \mathbf{M}_{\text{free}} \cdot \mathbf{M}_{\text{lens}_3} \cdot \mathbf{M}_{\text{free}_3} \cdot \mathbf{M}_{\text{tel}} \cdot \mathbf{M}_{\text{free}_1}$. As before, substituting the values of the matrix elements into Eq. (9) and Eq. (5) yields the intensity distribution of the light field after passing the lens system.

The beam profile at different propagation distances behind the last focusing lens is shown in Fig. 5. In order to get a good fitting between the calculated and measured intensity distributions, the theoretical distances have been simultaneously offset by 15 mm. This adjustment is justified since we neither measured the exact position of the chip of the CCD camera nor the precise focal length of each lens. Again we find very good agreement of experimental and theoretical curves. The beam profile at the focal plane of the last lens cannot be measured since the beam diameter at this position is too small to be resolved by the CCD camera.

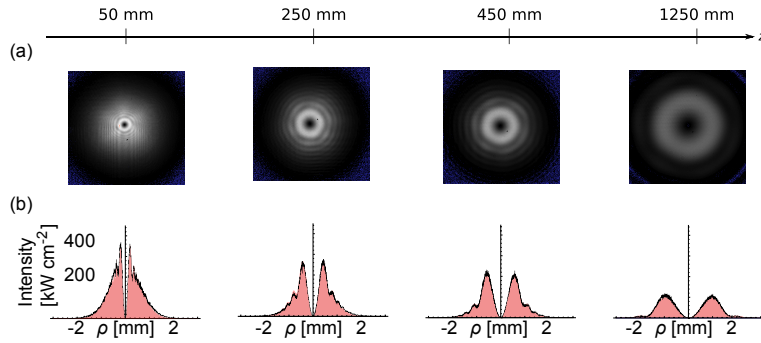


Fig. 4. (a) Intensity distributions of the SPP generated doughnut beam propagating in free space. The distribution at 250 mm is identical with Fig. 3. (b) One-dimensional radial intensity distributions with measured (black) and calculated (red) intensity distributions.

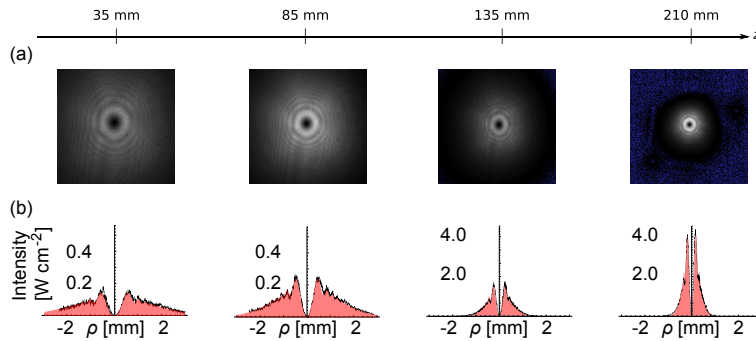


Fig. 5. (a) Intensity distributions of the SPP generated propagating doughnut beam transformed by the lens system at different propagation distances. (b) One-dimensional radial intensity distributions with measured (black) and calculated (red) intensity distributions.

4. Conclusion

We have shown that the analytic solution Eq. 9, which is easily evaluated with a computer, makes the propagation of SPP generated doughnut beams accessible by the *ABCD*-method. We expect the procedure to be relevant for many applications including optical microscopy, neutral atom trapping, optical tweezers, and propagation of optical angular momentum beams. Our results indicate that the slightly forgotten Collins-Huygens integral promises useful applications beyond the present SPP elements, e.g for the half-phase plates used in [3].

Acknowledgments

The authors acknowledge support by the Deutsche Forschungsgemeinschaft (FOR635 Quantum Control and Simulation with Distributed Systems of Atoms), and by the IP AQUITE of the European Commission. W. Alt is thanked for a critical reading of the manuscript.